

# Discovery of Novel Human Phenylethanolamine *N*-methyltransferase (hPNMT) Inhibitors Using 3D Pharmacophore-Based *in silico*, Biophysical Screening and Enzymatic Activity Assays

Dong-Il Kang<sup>1</sup>, Jee-Young Lee<sup>2,3</sup>, Woonghee Kim<sup>2,3</sup>, Ki-Woong Jeong<sup>2</sup>, Soyoung Shin<sup>2</sup>, Jiyoung Yang<sup>3</sup>, Eujin Park<sup>3</sup>, Young Kee Chae<sup>4</sup>, and Yangmee Kim<sup>2,3,\*</sup>

With the aid of receptor-oriented pharmacophore-based *in silico* screening, we established three pharmacophore maps explaining the binding model of hPNMT and a known inhibitor, SK&F 29661 (Martin et al., 2001). The compound library was searched using these maps. Nineteen selected candidate inhibitors of hPNMT were screened using STD-NMR and fluorescence experiments. An enzymatic activity assay based on HPLC was additionally performed. Consequently, three potential hPNMT inhibitors were identified, specifically, 4-oxo-1,4-dihydroquinoline-3,7-dicarboxylic acid, 4-(benzo[d][1,3]dioxol-5-ylamino)-4-oxobutanoic acid, and 1,4-diaminonaphthalene-2,6-disulfonic acid. These novel inhibitors were retrieved using Map II comprising one hydrogen bond acceptor, one hydrogen bond donor, one lipophilic feature, and shape constraints, including a hydrogen bond between Lys57 of hPNMT and a hydrogen bond donor of the inhibitor, and stacked hydrophobic interactions between the side-chain of Phe182 and an aromatic region of the inhibitor. Water-mediated interactions between Asn267 and Asn39 of hPNMT and the amide or amine group of three potent inhibitors were additional important features for hPNMT activity. The binding model presented here may be applied to identify inhibitors with higher potency. Moreover, our novel compounds are valuable candidates for further lead optimization of PNMT inhibitors.

## INTRODUCTION

*N*-methylation is a prominent pathway for the metabolism of several endogenous hormones and neurotransmitters. This reaction occurs via transfer of a methyl group from *S*-adenosyl-L-methionine (SAM) to nucleophilic amino groups, leading to the production of *N*-methylated metabolites and *S*-adeno-

syhomocysteine (SAH). Adrenaline (or epinephrine) accounts for 5–10% of total catecholamines in the central nervous system (CNS). Adrenaline is synthesized *in vivo* from noradrenaline in a reaction catalyzed by phenylethanolamine *N*-methyltransferase (PNMT), a 30 kDa enzyme that utilizes the cofactor SAM to methylate the amine of noradrenaline. PNMT is employed as a catecholamine biosynthetic marker, and the presence of PNMT-containing neurons in the brain suggests that CNS adrenaline is involved in the central control of blood pressure, respiration, and pituitary hormone secretion (Martin et al., 2001). It has been implicated in the effects of ethanol intoxication and neural degeneration observed in Alzheimer's disease (Kennedy et al., 2004; Mefford et al., 1990). There have been efforts to develop potent PNMT inhibitors as angina pectoris, myocardial infarction and anxiety neuroses agents (Comings, 2001; Križanova et al., 2007).

An extended series of investigations has focused on identifying effective substrates and inhibitors of hPNMT. The majority of these compounds are based on 1,2,3,4-tetrahydroisoquinoline and its analogues (Grunewald et al., 2005a; 2005b; 2006; 2007; 2008; Romero et al., 2004). Receptor-oriented pharmacophore-based *in silico* screening allows the systematic analysis of possible interactions between a large number of compounds and proteins, leading to the detection of noncovalent interactions in active sites of proteins (Fisher and Güner, 2002; Hoffrén et al., 2001; Kirchmair et al., 2001; 2007; McInnes, 2007). To identify novel and specific ligands, the active sites of proteins are analyzed for establishing pharmacophore maps, which depict sets of interactions (chemical features or functionalities) aligned in three-dimensional space, and include several features, along with excluded volume regions, based on the positions of receptor atoms (Elhallaoui et al., 2002; Pickett et al., 1996). For each library of compounds, a conformationally flexible database is constructed and searched with the set of pharmacophore maps. The resulting hits comprise

<sup>1</sup>Department of Chemistry, Konkuk University, Seoul 143-701, Korea, <sup>2</sup>Department of Bioscience and Biotechnology, Konkuk University, Seoul 143-701, Korea, <sup>3</sup>Bio/Molecular Informatics Center, Konkuk University, Seoul 143-701, Korea, <sup>4</sup>Department of Chemistry and Recombinant Protein Expression Center, Sejong University, Seoul 143-747, Korea

\*Correspondence: ymkim@kunkuk.ac.kr

Various conformers of a subset of compounds that satisfy one or more maps, and are thus expected to fit the active site reasonably well.

In our previous study, we performed a docking study for hPNMT and flavonoids, and suggested several interactions between hPNMT and its candidate inhibitors (Lee et al., 2009a). In this study, receptor-oriented pharmacophore-based *in silico* screening of hPNMT was performed to identify inhibitors of hPNMT. Candidate inhibitors were subsequently assessed for binding to hPNMT using biophysical screening methods, such as STD-NMR and fluorescence experiments. Enzymatic inhibition was further monitored by HPLC.

## MATERIALS AND METHODS

### Expression and purification of Hpnmt

hPNMT cDNA was a kind gift from the 21C Human Gene Bank, Genome Research Center, KRIBB, Korea. A hexa histidine-tagged hPNMT expression vector, pET-28a-hPNMT-His, was constructed by cloning into the *Bam*HI/*Xho*I restriction sites of pET-28a (Novagen, USA), and transformed into *E. coli* strain BL21. Cells were cultured at 30°C for 5 h prior to harvest by centrifugation, and resuspended in buffer comprising 20 mM Tris-HCl and 500 mM NaCl, pH 7.4 (buffer A). After sonication, lysed cells were centrifuged at 15,000 rpm for 20 min at 4°C to eliminate cellular debris. The supernatant was loaded onto a column packed with Ni-NTA resin (Amersham Biosciences, 5 ml). The resin was washed with 6 column volumes of buffer A containing 12.5 mM imidazole to eliminate weakly bound proteins. Elution buffer (buffer A containing 250 mM imidazole) was used for collecting hPNMT, which eluted as a sharp peak. The hPNMT fraction collected was subjected to gel filtration chromatography on a Superdex™ 75 column (Amersham Biosciences) with 10 mM Tris-HCl, 0.5 mM DTT, and 1.0 mM EDTA, pH 7.0, and collected hPNMT fraction was exchanged to buffer A. Purified hPNMT was identified with 10% SDS-PAGE, and protein purity assessed using MALDI-TOF mass spectrometry.

### Building of a 3D compound database

A 3D compound dataset was built with 200,000 synthetic compounds supported by Specs.net (Netherlands). Compounds were converted to 3D multiple conformers by Discovery Studio (DS) Catalyst DB Build module of the DS modeling 2.1 (Accelrys Inc., USA) (Lee et al., 2009a; 2009b; Taha et al., 2007). FAST method was used for multiple conformer generation that allowing 250 maximum conformers, and default values of all other parameters were applied.

### Receptor-oriented pharmacophore-based *in silico* screening of hPNMT

We defined the active site of hPNMT using the center and radius of the docked inhibitor, which based on the x-ray complex structure of hPNMT and a potent and selective PNMT inhibitor, SK&F 29661 (1HNN.pdb) and determined multiple pharmacophore maps (Martin et al., 2001). A list of features, including hydrogen bond donors (HBDs), hydrogen bond acceptors (HBAs) and lipophilicity (Lipo), were used to determine the pharmacophore map. Maps were generated with the excluded volume for heavy atoms, which is the forbidden area in the active site that defines its shape. To account for excluded volume regions occupied by heavy atoms in the receptor, an exclusion model was generated for the active site and surrounding receptor regions. Each atom of the receptor selected for inclusion in the model was presented as an exclusion point

(Hoffrén et al., 2001; Kirchhoff et al., 2001). Among these multiple pharmacophore maps, the most suitable one representing the binding model between hPNMT and inhibitor was established correctly via *in silico* screening with SK&F 29661. Pharmacophore maps that effectively expressed the binding model of enzyme with its inhibitors were selected for searching the compound library.

Using the final pharmacophore maps, we searched the Specs compound library and selected the candidates of hPNMT inhibitors based on visual inspection and estimation of the ligand score (LigScore) (Aparna et al., 2005; Venkatachalam et al., 2003). In particular, shape constraints were applied in database screening for regulating the number of hit compounds. These compounds were further subjected to medium-throughput screening. We performed all computational studies in a Linux environment using the DS modeling/SBP module (Accelrys Inc., USA) (Zou et al., 2008).

### HPLC enzymatic inhibition assay

Noradrenaline and adrenaline were separated using a Waters Atlantis™ dC18 4.6 × 250 mm, 5 μm column and Waters 2695 Alliance Separation Module. The mobile phase employed was H<sub>2</sub>O:acetonitrile:100 mM ammonium acetate, pH 5.0 = 10:2:88. The column temperature was maintained at 25°C, and a UV detector was monitored at 280 nm. To assess enzymatic inhibition, 125 μl of 20 μM hPNMT and 62.5 μl of 80 μM SAM were mixed thoroughly and incubated for 1 h at 37°C, followed by reaction with a DMSO stock (5 μl of 50 mM) of inhibitors for 15 min at 37°C. Noradrenaline (62.5 μl of 40 μM) was added and incubated for 15 min at 37°C. Reactions were terminated with 20 μl perchloric acid. The supernatant fractions were centrifuged at 6,000 rpm for 5 min, and 10 μl of sample solution was subsequently injected into the HPLC system maintained at 4°C and the chromatogram was monitored for 20 min. Final concentrations of hPNMT, SAM, inhibitor and noradrenaline were 10 μM, 20 μM, 1000 μM and 10 μM, respectively. The inhibition (%) was calculated by monitoring enhancement of the adrenaline peak as follows:

$$\text{Inhibition \%} = \left( 1 - \frac{\text{integral value of adrenaline of each samples}}{\text{integral value of adrenaline of control sample}} \right) \times 100$$

A control sample (with 100% of noradrenaline converted to adrenaline) was prepared under similar reaction conditions, but in the absence of inhibitor. The results were compared with those obtained with the commercially available hPNMT inhibitors, THIQ, 2-aminoindan (Grunewald et al, 1981; 2006). The dependence of percentage inhibition on inhibitor concentration was assessed by varying the concentrations of YPN010, YPN016, YPN017, THIQ and 2-aminoindan to 100, 250, 500, 750 and 1000 μM. The time dependence of percentage inhibition was monitored against various reaction times (ranging from 8 to 180 min) with YPN010 and THIQ at a fixed concentration of 500 μM.

### NMR screening

Saturation transfer difference (STD) NMR have been widely used for the study of protein-ligand interaction. Information can be gained quickly and easily with these techniques. They need only small amounts of non-isotope-labeled, and thus readily available, target macromolecules (Meyer and Peters, 2003). STD-NMR was performed at KBSI (Korea Basic Science Institute) to identify the inhibitors bound to PNMT. Spectra were collected from regions containing only protein resonances at 298 K, both with and without saturation (Macnaughtan et al.,

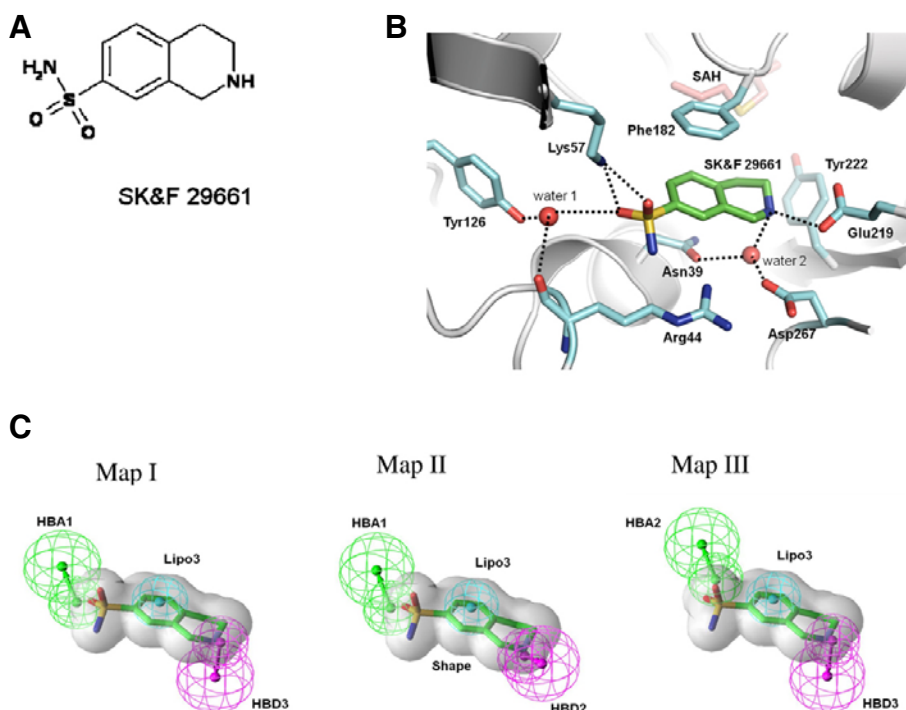


**Fig. 1.** Interaction model and three pharmacophore maps of hPNMT. (A) 2D structure of SK&F 29661. (B) Interaction model of hPNMT and inhibitor SK&F 29661 from x-ray complex structure (1HNN.pdb). Black dashed-line indicates hydrogen bonding interaction. (C) Three pharmacophore maps which derived from hPNMT. Green: hydrogen bond acceptor, Magenta: hydrogen bond donor, Cyan: lipophilic features.

2006; Mayer and Meyer, 2001). In the presence of excess ligand, spectral differences primarily constituted resonances belonging to ligand protons bound to PNMT. The protein was saturated on-resonance at -1.0 ppm and off-resonance at 40 ppm, with a cascade of 40 selective Gaussian-shaped pulses of 50 ms duration and a 100  $\mu$ s delay between each pulse in all STD-NMR experiments. The total duration of the saturation time was set to 2 s.

For STD-NMR experiments, 10  $\mu$ M recombinant hPNMT in 10 mM Tris-Cl, 0.5 mM DTT, pH 7.0, and 1.0 mM of each candidate inhibitor was added (protein:ligand ratio of 1:100). In total, 1024 scans for each STD-NMR experiment were acquired, and a WATERGATE sequence used to suppress the water signal. A spin-lock filter (5 kHz strength and 10 ms duration) was applied to suppress the protein background.

### Fluorescence analysis

The hPNMT protein (10  $\mu$ M) was added to buffer (20 mM Tris-HCl, 500 mM NaCl, pH 7.4, and 20  $\mu$ M SAM). Each inhibitor candidate (YPN010, YPN016, YPN017) and THIQ was titrated to a final protein:inhibitor ratio of 1:10. The sample was contained in a 2 ml thermostatted cuvette with excitation and emission path lengths of 10 mm. Fluorescence quantum yields of hPNMT and ligand were determined by tryptophan emission. Samples were excited at 290 nm, and emission spectra were recorded for light scattering effects from 290 to 500 nm. We estimated  $K_d$  using the following equation (Mishra et al., 2005):

$$\log\left(\frac{F_0 - F}{F}\right) = \log\frac{1}{K_d} + n\log[inhibitor]$$

$F_0$  and  $F$  represent fluorescence intensity from hPNMT at 342 nm in the absence and presence of inhibitor, respectively, while  $n$  is the number of inhibitor binding sites on the protein.

## RESULTS

### In silico screening of Hpnmt

The 3D structure of hPNMT was obtained from the PDB entry, 1HNN. The geometric center of the hPNMT inhibitor was used to define the active site center. The 10.0 Å radius includes all the residues forming the first shell around SK&F 29661 bound to the receptor. The three-dimensional structure of hPNMT and model of binding to its inhibitor (SK&F 29661) are presented in Fig. 1. Chemical features were generated from receptor atoms within 10.0 Å from the active site center, and organized into three donors, three acceptors, and five lipophilic clusters.

Several inhibitors of hPNMT accept hydrogen bonds directly or often via a water molecule, with Lys57, Glu219 and Asp267 of hPNMT (Gee et al., 2005; Krovat et al., 2005). Based on this information, each receptor-based pharmacophore map is composed of three features and shape constraints to regulate the number of hit compounds (Fisher and Güner, 2002; Pickett et al., 1996). In total, 165 receptor-based multiple pharmacophore maps were generated using all possible combinations of the three features.

Among the 165 maps, only three represented the binding model of hPNMT and SK&F 29661 effectively, as shown in Fig. 1(C). Two hydrogen bond acceptors, HBA1 and HBA2, correspond to the potential hydrogen bonding site of the Lys57 side-chain. Two hydrogen bond donors, HBD2 and HBD3, correspond to the potential hydrogen bonding site between the Glu219 side-chain and a water molecule. Each map is composed of one HBA, one HBD, one Lipo feature and shape constraints. The three maps were used to search a database built with 200,000 compounds. Consequently, we selected 17 potential candidate hPNMT inhibitors, based on visual inspection and ligand score (LigScore) (Rambabu et al., 2005; Venkatachalam et al., 2003). Two-dimensional structures and their LigScores are presented in Table 1. We expected the highly ranked compounds, such as YPN010, YPN016 and YPN017,

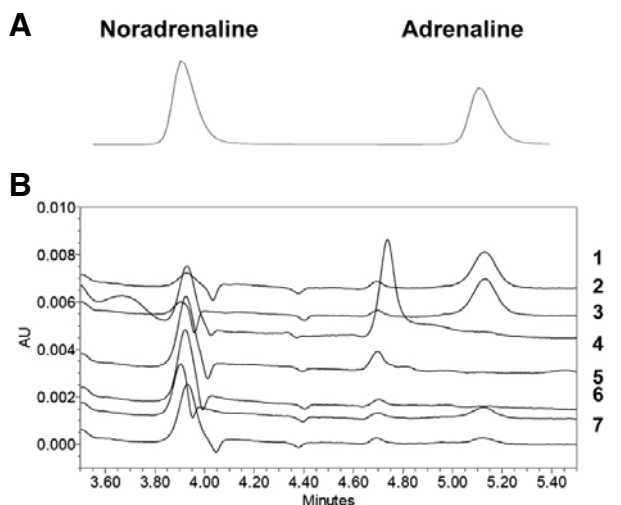


**Fig. 2.** (A) HPLC separation of noradrenaline and adrenaline. (B) Stacked chromatograms of representative HPLC inhibition assays. 1. Control, 2. YPN005, 3. YPN017, 4. YPN016, 5. YPN010, 6. THIQ, 7. 2-aminoindan.

to account for maximal binding affinity to hPNMT, compared with the remaining 14 compounds. The selected compounds had similar molecular sizes as a result of shape constraints, and the center of each molecule contained a hydrophobic site due to the Lipo feature. These compounds were further subjected to medium-throughput screening.

#### HPLC enzymatic activity assay

To verify the virtual screening results, we monitored the conversion of noradrenaline to adrenaline in the presence of hPNMT, SAM and each inhibitor. hPNMT was purified to a high purity as confirmed using SDS-PAGE and MALDI-TOF mass spectrometry. Previously, Borchardt et al. (Borchardt et al., 1977) developed a liquid chromatographic assay for hPNMT using a cation-exchange resin and an electrochemical detector. However, most PNMT assays to date have been performed via liquid scintillation with expensive  $^{14}\text{C}$ - or  $^3\text{H}$  isotope-labeled SAM (Grunewald et al., 1999; 1981; McInnes, 2007). In this study, we employ HPLC separation using a C18 column and UV detector, analogous to the Borchardt method, to assess enzymatic inhibition. Noradrenaline and adrenaline are polar compounds, and thus difficult to retain on a reversed-phase HPLC column, and high water ratio in the mobile phase was required. Waters Atlantis<sup>TM</sup>, a silica-based line of difunctionally bonded reversed-phase C<sub>18</sub> columns, was used in the mobile phase, as described in Materials and methods. Since the conversion of noradrenaline to adrenaline is an irreversible process, percentage inhibition is dependent on the time taken for the assay. Despite our attempts to fix the reaction time to 15 min at 37°C, small variations in time and reaction temperature, along with other parameters, may have influenced the results. These possible errors were corrected by comparing the HPLC area with a control sample containing only DMSO with no inhibitor. We assume that the control sample converts 100% of noradrenaline to adrenaline.

The HPLC assay method was applied to known commercially available inhibitors (THIQ and 2-aminoindan), as well as the 17 candidates identified by *in silico* screening. As shown in Figs. 2 and 3, YPN010, YPN016 and YPN017 completely suppressed the conversion of noradrenaline to adrenaline, while

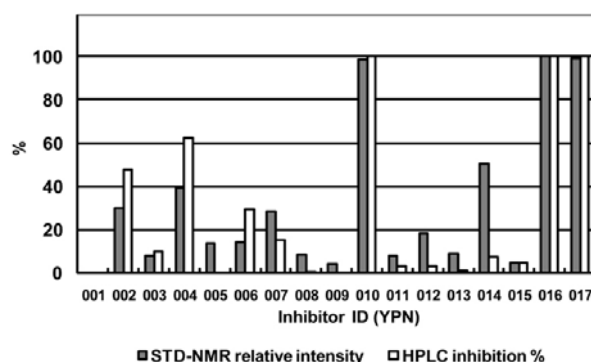


**Fig. 3.** Comparison of STD-NMR and HPLC assay data. The STD-NMR peak intensity was compared to the most intensive peak (YPN016).

YPN002, YPN004, YPN006 and YPN007 displayed moderate (20% to 80%) inhibitory activity. This suppression of hPNMT-induced N-methylation provides evidence that YPN010, YPN016 and YPN017 bind to the active site of hPNMT and compete with noradrenaline. Results obtained with YPN010, YPN016 and YPN017 were in agreement with LigScore data (Table 1). THIQ and 2-aminoindan displayed slightly lower inhibitory activity (88%) than YPN010, YPN016 and YPN017.

The dependence of inhibitor activity on concentration and reaction time are presented in Fig. 4. In both cases, the YPN series displayed slightly stronger inhibitory behavior than THIQ.

#### Biophysical screening using NMR spectroscopy

STD-NMR spectra contained resonances specific for YPN016 bound to PNMT, but no peaks representing YPN008 (Figs. 5A and 5B). HPLC and NMR results are compared in Fig. 3. STD-NMR peaks of YPN010, YPN016 and YPN017 binding well with hPNMT and have similar intensities, in agreement with the HPLC results (100% inhibition). Despite significant differences between the two screening methods employed, both yielded consistent data, further confirming the accuracy of these techniques.

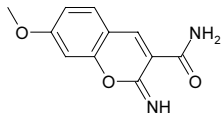
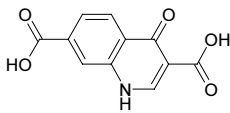
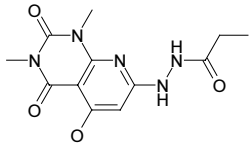
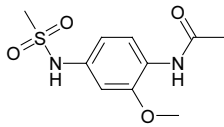
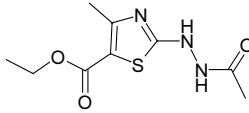
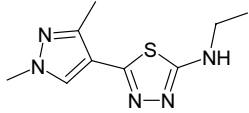
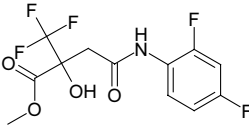
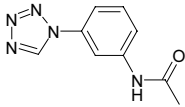
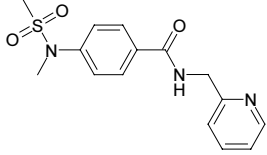
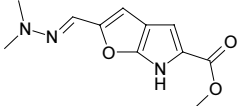
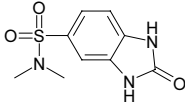
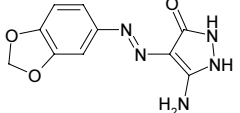
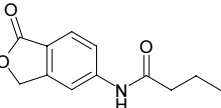
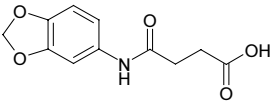
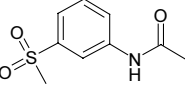
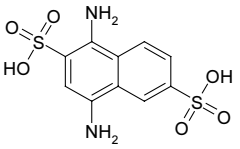
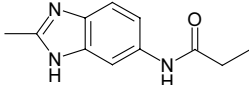
#### Fluorescence studies and dissociation constants

The hPNMT protein contains six tryptophan residues (positions 56, 113, 123, 140, 221, and 276). Among these, Trp221 is close to the binding site. In the presence of inhibitors, protein fluorescence was decreased. This quenching of fluorescence was used to estimate the binding constant. Binding (or dissociation) constant,  $K_d$ , is defined as  $[\text{free protein}][\text{free inhibitor}]/[\text{complex}]$  (Möller and Denicola, 2002; Park et al., 2008). The fluorescence intensity was altered with increasing inhibitor concentrations. These changes are attributed to the formation of a complex of protein and inhibitor. The  $K_d$  values for the three novel inhibitors, YPN010, YPN016 and YPN017, are  $0.86 \pm 0.014 \mu\text{M}$ ,  $0.32 \pm 0.042 \mu\text{M}$  and  $0.12 \pm 0.021 \mu\text{M}$ , respectively. These candidates are at least five thousand fold stronger than THIQ which has the  $K_d$  value of  $7.28 \pm 0.26 \text{ mM}$ . The binding affinity of potential candidate inhibitors are listed in Table 2.

#### DISCUSSION

SAM-dependent methyl transfer is one of the most extensive physiological reactions. Among the methyltransferases, PNMT participates in the terminal step of adrenaline synthesis from noradrenaline, and is used as a catecholamine biosynthetic

**Table 1.** Structures of candidate inhibitors of hPNMT and LigScores

Compound	Structure	LigScore	Compound	Structure	LigScore
YPN001		11.75	YPN010		12.49
YPN002		5.72	YPN011		8.16
YPN003		6.19	YPN012		6.39
YPN004		6.58	YPN013		10.28
YPN005		5.80	YPN014		6.86
YPN006		7.97	YPN015		11.91
YPN007		7.46	YPN016		13.22
YPN008		6.52	YPN017		12.23
YPN009		10.62			

marker and regulator of the central nervous system. We attempted to screen for effective inhibitors of hPNMT using a 3D pharmacophore model with a structure-based focusing approach. Among the three multiple pharmacophore maps generated, Map II predicted interactions between inhibitors and hPNMT in accordance with experimental results. Our data confirm that Lys57 and water molecules represent important fea-

tures for hPNMT activity, and consequently, three novel inhibitors were identified. The  $K_d$  values for the three novel inhibitors, YPN010, YPN016 and YPN017, are  $0.86 \pm 0.014 \mu\text{M}$ ,  $0.32 \pm 0.042 \mu\text{M}$  and  $0.12 \pm 0.021 \mu\text{M}$ , respectively.

A combination of *in silico* analysis using the structure-based 3D pharmacophore system and medium-throughput biophysical screening is a useful tool for the identification of selective

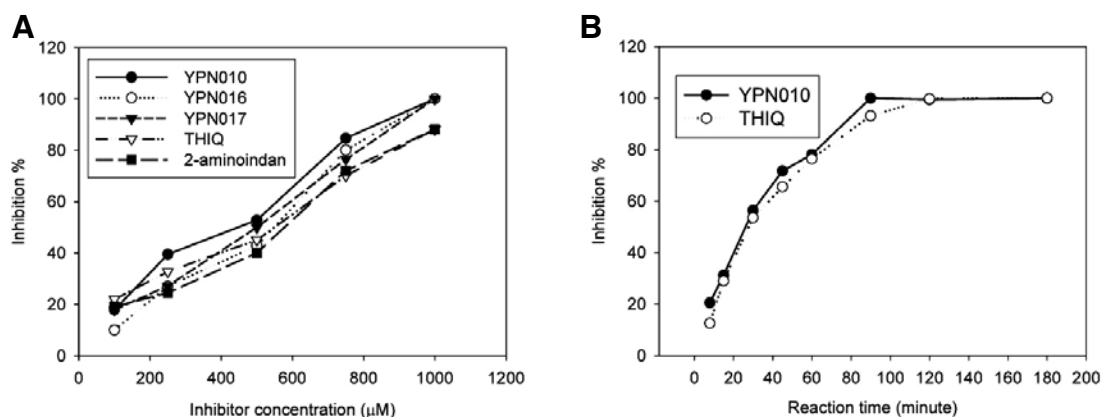


**Fig. 4.** The dependence of (A) concentration of inhibitors and (B) reaction time. YPN series displayed slightly stronger inhibitory behavior than THIQ and 2-aminoindan.

**Table 2.** Binding affinity of candidate inhibitors of hPNMT

Compound	$K_d$ ( $\mu$ M)
THIQ	$7280 \pm 260$
YPN010	$0.86 \pm 0.014$
YPN016	$0.32 \pm 0.042$
YPN017	$0.16 \pm 0.021$

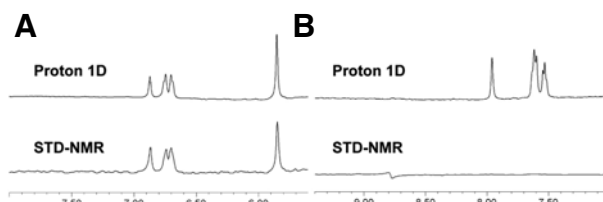


**Fig. 5.** Representative results of the STD-NMR binding assay. (A) YPN016 displayed 100% inhibitory activity, while (B) YPN008 promoted 0% inhibition in the HPLC enzymatic inhibition assay.

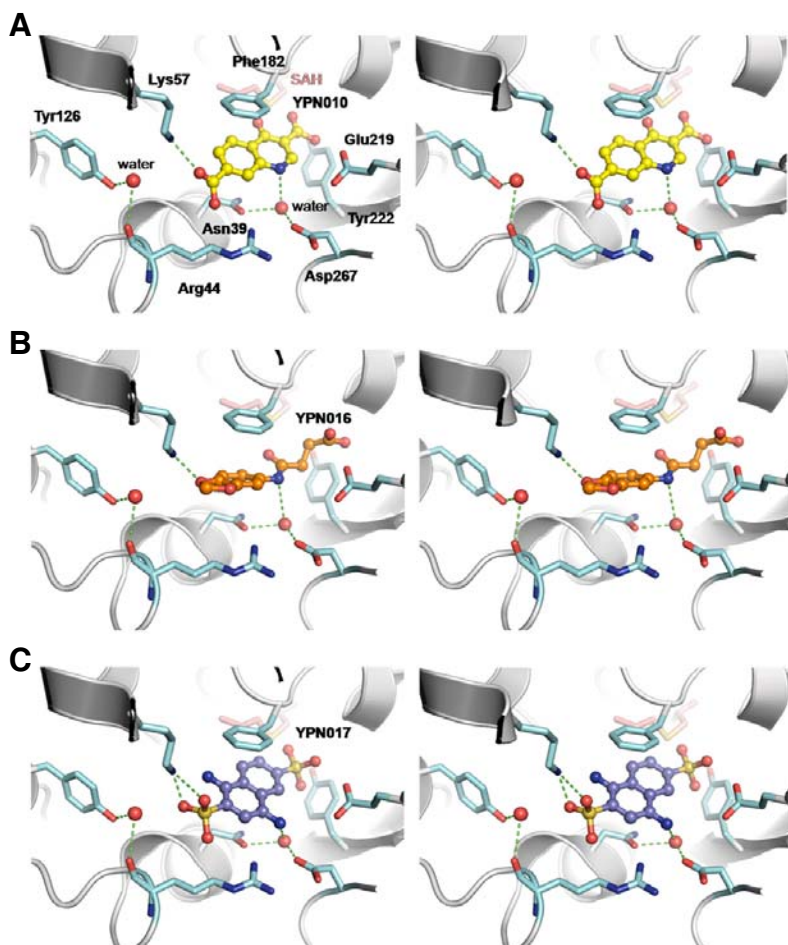


**Fig. 6.** Stereo views of interaction model of (A) YPN010, (B) YPN016 and (C) YPN017 at the active site of hPNMT. Hydrogen bonds are included in the docking model of inhibitors and hPNMT.

ligands for specific receptors. Here, we employ these techniques to effectively detect specific inhibitors of CNS-activated hPNMT. HPLC-based assays of inhibition of N-methylation catalysis by hPNMT provide clear evidence that YPN010, YPN016 and YPN017 bind to the active site of the protein and compete with noradrenaline. STD-NMR technique was an efficient tool to identify the inhibitors of hPNMT and fluorescence experiments were useful to measure the binding affinity of the compounds without radioisotope labeling. The combination approach described here may be generally applicable for the identification of inhibitors of protein-ligand interactions, which would facilitate an increase in the number of therapeutic targets accessible for intervention.

Three new potent inhibitors, 4-oxo-1,4-dihydroquinoline-3,7-dicarboxylic acid (YPN010), 4-(benzo[d][1,3]dioxol-5-ylamino)-4-oxobutanoic acid and 1,4-diaminonaphthalene-2,6-disulfonic acid (YPN017), confirmed by enzymatic activity assays and biophysical screening, were retrieved using pharmacophore Map II. As mentioned earlier, Map II represents interactions with Lys57 and a water molecule. A binding model of YPN010 and hPNMT is depicted in Fig. 6. Hydroxyl group of the benzoic acid moiety in YPN010 participates in hydrogen bonding with a side-chain of Lys57. A nitrogen atom on the quinoline ring in YPN010 also forms a hydrogen bond with a water molecule, which simultaneously forms a hydrogen bond with Asn39 and Asp267. Gee et al. (2005) reported particularly strong water-mediated interactions of  $\beta$ -hydroxyl of (R)-*p*-octopamine with Asp267. These interactions are conserved in YPN010, YPN016 and YPN017 by amide or amine groups, in lieu of  $\beta$ -hydroxyl, as shown in Fig. 6. An oxygen atom on the benzodioxole ring of YPN016, and sulfonyl oxygen of sulfonic acid and hydrogen atom of the amine group in YPN017 participate in hydrogen bonding with Asn39 and Asp267 in hPNMT, respectively. Thus, it appears that pharmacophore Map II suitably represents interactions between hPNMT and inhibitors.

A cryptic binding site of hPNMT was identified by the group of J.L. Martin (Gee et al., 2007). Their results indicate that the conformation of a side-chain of Lys57 is perturbed, and no longer participates in direct interactions with inhibitor. Moreover, three active site residues were reported as flexible (Lys57, Cys60, and Tyr126), which affected the docking model of inhibitors. However, the authors confirmed a crucial role of Lys57 in the activity of hPNMT consistent with earlier reports. We have successfully identified inhibitors with our model, verified by biophysical screening, which provides additional evidence that Lys57 plays an important role, at least in the early stage of ligand binding to hPNMT. We will further attempt to screen inhibitors with a model considering side-chain flexibility in the active site. Here, we specifically report a case of screening that involves interactions with Lys57.

Our *in silico* screening and biological activity findings are significantly correlated. If we consider that these compounds are only first-round hPNMT hits discovered by virtual screening, the binding model presented in this study may be effectively applied to discover inhibitors of higher potency. Moreover, our novel compounds may be valuable candidates for further lead optimization of PNMT inhibitors.

## ACKNOWLEDGMENTS

This work was supported by Konkuk University in 2010.

## REFERENCES

Aparna, V., Rambabu, G., Panigrahi, S.K., Sarma, J.A., and Desiraju, G.R. (2005). Virtual screening of 4-anilinoquinazoline analogues as EGFR kinase inhibitors: importance of hydrogen

- bonds in the evaluation of poses and scoring functions. *J. Chem. Inf. Model.* **45**, 725-738.
- Borchardt, R.T., Vincek, W.C., and Grunewald, G.L. (1997). A liquid chromatographic assay for phenylethanolamine N-methyltransferase. *Anal. Biochem.* **242**, 149-157.
- Comings, D.E. (2001). Clinical and molecular genetics of ADHD and Tourette syndrome. Two related polygenic disorders. *Ann. N. Y. Acad. Sci.* **931**, 50-83.
- Elhallaoui, M., Laguerre, M., Carpy, A., and Ouazzani, F.C. (2002). Molecular modeling of noncompetitive antagonists of the NMDA receptor: proposal of a pharmacophore and a description of the interaction mode. *J. Mol. Model.* **8**, 65-72.
- Fisher, L.S., and Güner, O.F. (2002). Seeking Novel Leads through Structure-based pharmacophore design. *J. Braz. Chem. Soc.* **23**, 777-787.
- Gee, C.L., Tyndall, J.D., Grunewald, G.L., Wu, Q., McLeish, M.J., and Martin, J.L. (2005). Mode of binding of methyl acceptor substrates to the adrenaline-synthesizing enzyme phenylethanolamine N-methyltransferase: implications for catalysis. *Biochemistry* **44**, 16875-16885.
- Grunewald, G.L., Borchardt, R.T., Rafferty M.F., and Krass, P. (1981). Conformational preferences of amphetamine analogues for inhibition of phenylethanolamine N-methyltransferase. Conformationally defined adrenergic agents. *Mol. Pharmacol.* **20**, 377-381.
- Grunewald, G.L., Dahanukar, V.H., Teoh, B., and Criscione, K.R. (1999). 3,7-Disubstituted-1,2,3,4-tetrahydroisoquinolines display remarkable potency and selectivity as inhibitors of phenylethanolamine N-methyltransferase versus the  $\alpha_2$ -adrenoceptor. *J. Med. Chem.* **42**, 1982-1990.
- Grunewald, G.L., Lu, J., Criscione, K.R., and Okoro, C.O. (2005a). Inhibitors of phenylethanolamine N-methyltransferase devoid of  $\alpha_2$ -adrenoceptor affinity. *Bioorg. Med. Chem. Lett.* **15**, 5319-5323.
- Grunewald, G.L., Romero, F.A., and Criscione, K.R. (2005b). Nanomolar inhibitors of CNS epinephrine biosynthesis: (R)-(+)-3-fluoromethyl-7-(N-substituted aminosulfonyl)-1,2,3,4-tetrahydroisoquinolines as potent and highly selective inhibitors of phenylethanolamine N-methyltransferase. *J. Med. Chem.* **48**, 1806-1812.
- Grunewald, G.L., Seim, M.R., Regier, R.C., Martin, J.L., Gee, C.L., Drinkwater, N., and Criscione, K.R. (2006). Comparison of the binding of 3-fluoromethyl-7-sulfonyl-1,2,3,4-tetrahydroisoquinolines with their isosteric sulfonamides to the active site of phenylethanolamine N-methyltransferase. *J. Med. Chem.* **49**, 5424-5433.
- Grunewald, G.L., Seim, M.R., Regier, R.C., and Criscione, K.R. (2007). Exploring the active site of phenylethanolamine N-methyltransferase with 1,2,3,4-tetrahydrobenz[*h*]isoquinoline inhibitors. *Bioorg. Med. Chem.* **15**, 1298-1310.
- Grunewald, G.L., Seim, M.R., Bhat, S.R., Wilson, M.E., and Criscione, K.R. (2008). Synthesis of 4,5,6,7-tetrahydrothieno[3,2-*c*]pyridines and comparison with their isosteric 1,2,3,4-tetrahydroisoquinolines as inhibitors of phenylethanolamine N-methyltransferase. *Bioorg. Med. Chem.* **16**, 542-559.
- Hoffrén, A.M., Murray, C.M., and Hoffmann, R.D. (2001). Structure-based focusing using pharmacophores derived from the active site of 17 $\beta$ -hydroxysteroid dehydrogenase. *Curr. Pharm. Des.* **7**, 547-566.
- Kennedy, B.P., Bottiglieri, T., Arning, E., Ziegler, M.G., Hansen, L.A., and Masliah, E. (2004). Elevated S-adenosylhomocysteine in Alzheimer brain: influence on methyltransferases and cognitive function. *J. Neural Transm.* **111**, 547-567.
- Kirchhoff, P.D., Brown, R., Kahn, S., Waldman, M., and Venkatachalam, C.M. (2001). Application of structure-based focusing to the estrogen receptor. *J. Comp. Chem.* **22**, 993-1003.
- Kirchmair, J., Ristic, S., Eder, K., Markt, P., Wolber, G., Laggner, C., and Langer T. (2007). Fast and Efficient *in Silico* 3D Screening: Toward Maximum Computational Efficiency of Pharmacophore-Based and Shape-Based Approaches. *J. Chem. Inf. Model.* **47**, 2182-2196.
- Krizanova, O., Myslivecek, J., Tillinger, A., Jurkovicova, D., and Kubovcakova, L. (2007). Adrenergic and calcium modulation of the heart in stress: From molecular biology to function. *Stress* **10**, 173-184.
- Krovat, E.M., Frühwirth, K.H., and Langer, T. (2005). Pharmacophore identification, *in silico* screening, and virtual library de-

- sign for inhibitors of the human factor Xa, *J. Chem. Inf. Model.* **45**, 146-159.
- Lee, J.Y., Jeong, K.W., and Kim, Y. (2009a). Flavonoids can be potent inhibitors of human phenylethanolamine N-methyltransferase (hPNMT). *Bull. Korean Chem. Soc.* **30**, 1835-1838.
- Lee, J.Y., Jeong, K.W., Lee, J.U., Kang, D.I., and Kim, Y. (2009b). Novel *E. coli* beta-ketoacyl-acyl carrier protein synthase III inhibitors as targeted antibiotics. *Bioorg. Med. Chem.* **17**, 1506-1513.
- Macnaughtan, M.A., Kamar, M., Alvarez-Manilla, G., Venot, A., Glushka, J., Pierce, J.M., and Prestegard, J.H. (2006). NMR structural characterization of substrates bound to N-acetyl-glucosaminyltransferase V. *J. Mol. Biol.* **366**, 1266-1281.
- Martin, J.L., Begun, J., McLeish, M.J., Caine, J.M., and Grunewald, G.L. (2001). Getting the adrenaline going: crystal structure of the adrenaline-synthesizing enzyme PNMT. *Structure* **9**, 977-985.
- Mayer, M., and Meyer, B. (2001). Group epitope mapping by saturation transfer difference NMR to identify segments of a ligand in direct contact with a protein receptor. *J. Am. Chem. Soc.* **123**, 6108-6117.
- McInnes, C. (2007). Virtual screening strategies in drug discovery. *Curr. Opin. Chem. Biol.* **11**, 494-502.
- Mefford, I.N., Lister, R.G., Ota, M., and Linnoila, M. (1990). Antagonism of ethanol intoxication in rats by inhibitors of phenylethanolamine N-methyltransferase, *Alcohol Clin. Exp. Res.* **14**, 53-57.
- Meyer, B., and Peters T. (2003). NMR spectroscopy techniques for screening and identifying ligand binding to protein receptors. *Angew. Chem. Int. Ed. Engl.* **42**, 864-890.
- Mishra, B., Barik, A., Priyadarsini, K.I., and Mohan, H. (2005). Fluorescence spectroscopic studies on binding of a flavonoid antioxidant quercetin to serum albumins. *J. Chem. Sci.* **117**, 641-647.
- Möller, M., and Denicola, A. (2002). Study of protein-ligand binding by fluorescence. *Biochem. Mol. Biol. Edu.* **30**, 309-312.
- Park, H., Pack, C., Kinjo, M., and Kaang, B.K. (2008). *In vivo* quantitative analysis of PKA subunit interaction and cAMP level by dual color fluorescence cross correlation spectroscopy. *Mol. Cells* **26**, 87-92.
- Pickett, S.D., Mason, J.S., and McLay, I.M. (1996). Diversity profiling and design using 3D pharmacophores: Pharmacophore-Derived Queries (PDQ). *J. Chem. Inf. Comput. Sci.* **36**, 1214-1223.
- Romero, F.A., Vodonick, S.M., Criscione, K.R., McLeish, M.J., and Grunewald, G.L. (2004). Inhibitors of phenylethanolamine N-methyltransferase that are predicted to penetrate the blood-brain barrier: design, synthesis, and evaluation of 3-fluoromethyl-7-(N-substituted aminosulfonyl)-1,2,3,4-tetrahydroisoquinolines that possess low affinity toward the  $\alpha_2$ -adrenoceptor, *J. Med. Chem.* **47**, 4483-4493.
- Taha, M.O., Bustanji, Y., Al-Bakri, A.G., Yousef, A.M., Zalloum, W.A., Al-Masri, I.M., and Atallah, N. (2007). Discovery of new potent human protein tyrosine phosphatase inhibitors via pharmacophore and QSAR analysis followed by in silico screening. *J. Mol. Graph. Model.* **25**, 870-884.
- Venkatachalam, C.M., Jiang, X., Oldfield, T., and Waldman, M. (2003). LigandFit: a novel method for the shape-directed rapid docking of ligands to protein active sites. *J. Mol. Graph. Model.* **21**, 289-307.
- Zou, J., Xie, H.Z., Yang, S.Y., Chen, J.J., Ren, J.X., and Wei, Y.Q. (2008). Towards more accurate pharmacophore modeling: Multicomplex-based comprehensive pharmacophore map and most-frequent-feature pharmacophore model of CDK2. *J. Mol. Graph. Model.* **27**, 430-438.